Journal of Physics and Chemistry of Solids 69 (2008) 2514–2519

Contents lists available at ScienceDirect

Journal of Physics and Chemistry of Solids

journal homepage: www.elsevier.com/locate/jpcs

Effect of heat treatment on the optical and electrical transport properties of $Ge_{15}Sb_{10}Se_{75}$ and $Ge_{25}Sb_{10}Se_{65}$ thin films

K.A. Aly [a,*], M.A. Osman [b], A.M. Abousehly [a], A.A. Othman [b]

[a] Department of Physics, Faculty of Science, Al-Azhar University, Assiut, Egypt
[b] Department of Physics, Assiut University, Assiut, Egypt

ARTICLE INFO

Article history:
Received 11 November 2007
Received in revised form
21 March 2008
Accepted 7 May 2008

Keywords:
C. Differential scanning calorimetry (DSC)
C. X-ray diffraction
D. Optical properties

ABSTRACT

The effect of heat treatment on the optical and electrical properties of $Ge_{15}Sb_{10}Se_{75}$ and $Ge_{25}Sb_{10}Se_{65}$ thin films in the range of annealing temperature 373–723 K has been investigated. Analysis of the optical absorption data indicates that Tauc's relation for the allowed non-direct transition successfully describes the optical processes in these films. The optical band gap ($E_g^{opt.}$) as well as the activation energy for the electrical conduction (ΔE) increase with the increase of annealing temperature (T_a) up to the glass transition temperature (T_g). Then a remarkable decrease in both the $E_g^{opt.}$ and ΔE values occurred with a further increase of the annealing temperature ($T_a > T_g$). The obtained results were explained in terms of the Mott and Davis model for amorphous materials and amorphous to crystalline structure transformations. Furthermore, the deduced value of $E_g^{opt.}$ for the $Ge_{25}Sb_{10}Se_{65}$ thin film is higher than that observed for the $Ge_{15}Sb_{10}Se_{75}$ thin film. This behavior was discussed on the basis of the chemical ordered network model (CONM) and the average value for the overall mean bond energy $\langle E \rangle$ of the amorphous system $Ge_xSb_{10}Se_{90-x}$ with $x = 15$ and 25 at%. The annealing process at $T_a > T_g$ results in the formation of some crystalline phases GeSe, $GeSe_2$ and Sb_2Se_3 as revealed in XRD patterns, which confirms our discussion of the obtained results.

1. Introduction

Chalcogenide glasses are well known for their IR-transmitting characteristics [1]. They exhibit a wide range of photo-induced effects accompanied by significant changes in their optical properties, which enable them to be used as an optical recording, imaging media [2] and absorption filters [3]. Studying the optical and electrical properties of amorphous materials has achieved great attention due to their interesting technological applications [4,5]. The common feature of these glasses is the presence of localized states in the mobility gap as a result of the absence of long-range order as well as various inherent defects. The optical properties of amorphous solid are determined by the structural bonding between neighboring atoms. The structural bonding is not highly stable and several factors [6] such as heat treatment, incident light and electric field are found to induce the transition. Physico-chemical and optical properties of the Ge–Sb–Se system were studied elsewhere [7–10]. Also, the elastic properties [11], the thermal analysis [12] and the compositional effects on the optical and thermal diffusivity of bulk $Ge_xSb_5Se_{95-x}$ glasses have been studied [13]. Furthermore, the effect of Sb content and heat treatment on the optical [14,15], electrical and thermal properties of $Ge_{20}Sb_xSe_{80-x}$ has been investigated [16].

The heat treatment process plays an important role in inducing crystallization in amorphous semiconductor and chalcogenide thin films [17]. Crystallization of chalcogenide films due to the annealing of these films at temperatures (T_a) higher than its glass transition temperature (T_g) is accompanied by decrease in the value of the optical band gap ($E_g^{opt.}$) and the activation energy for electrical conduction (ΔE) [18,19], while the contrary was observed by annealing these films at temperatures less than or equal to the glass transition temperature [20–23]. The aim of this work is to study the effect of annealing process on the optical and electrical properties of $Ge_{15}Sb_{10}Se_{75}$ and $Ge_{25}Sb_{10}Se_{65}$ thermally evaporated films.

2. Experimental details

Amorphous $Ge_{15}Sb_{10}Se_{75}$ and $Ge_{25}Sb_{10}Se_{65}$ bulk samples were prepared from Ge, Sb and Se elements of high purity (5N) by the usual melt quench technique. Thin films of these chalcogenides were prepared by thermal evaporation onto cleaned glass substrates. The thermal evaporation process was carried out in a coating system Denton Vacuum (DV-502A) at a pressure of

* Corresponding author. Tel./fax: +20 882325647.
E-mail address: kamalaly2001@Gmail.com (K.A. Aly).

0022-3697/$ - see front matter Crown Copyright © 2008 Published by Elsevier Ltd. All rights reserved.
doi:10.1016/j.jpcs.2008.05.003

approximately 1×10^{-5} Torr. The temperature of the substrates was kept at room temperature during the deposition process. The film thickness was controlled using a thickness monitor Denton's model DTM-100. The chemical compositions of $Ge_{15}Sb_{10}Se_{75}$ and $Ge_{25}Sb_{10}Se_{65}$ films were checked by using energy dispersive X-ray spectroscopy (EDXS). The X-ray diffraction (XRD) patterns for the as-deposited and annealed films were carried out by using an X-ray diffractometer (Philips type 1710 with Cu as a target and Ni as a filter, $\lambda = 1.5418$ Å). The calorimetric measurements were carried out by using a calibrated differential scanning calorimeter DSC (Shimadzu 50) with an accuracy of 0.1 K, keeping a constant flow of nitrogen to extract the gases generated during the crystallization reactions, characteristic of chalcogenide materials. About 15 mg powdered samples were introduced into aluminum pans and scanned over the temperature range 300–750 K at continuous heating rates of 10 K/min.

The optical transmittance and reflectance for the as-deposited and annealed (under vacuum approximately 2.66×10^{-3} Torr) $Ge_{15}Sb_{10}Se_{75}$ and $Ge_{25}Sb_{10}Se_{65}$ thin films have been measured at the wavelength range 400–900 nm using the Shimadzu 2101 UV–Vis. double beam spectrophotometer. The refractive index (n) and extinction absorption coefficient (k) were computed through the fitting of the obtained spectra to the exact expressions for the transmittance and reflectance of the multi-large structure given by

$$|T(n,k,d,\lambda) - T_{exp}(\lambda)|^2 = (\Delta T)^2 \quad (1)$$

$$|R(n,k,d,\lambda) - R_{exp}(\lambda)|^2 = (\Delta R)^2 \quad (2)$$

where T (n, k, d, λ) and R (n, k, d, λ) are the calculated values of T and R using Murman's exact equations [24,25], $T_{exp}(\lambda)$ and $R_{exp}(\lambda)$ are the experimental measured values of T and R, respectively, k is the extinction coefficient and n is the refractive index. The absorption coefficient (α) for the investigated films was calculated using the well-known expression ($\alpha = 4\pi k/\lambda$), and then the values of the optical band gap $E_g^{opt.}$ were obtained from the intercept of $(\alpha h\nu)^{1/2}$ versus hν at $(\alpha h\nu)^{1/2} = 0$, according to Tauc's relation for the allowed non-direct optical transition [26,27].

$$(\alpha h\nu)^{1/2} = B\,(h\nu - E_g^{opt.}) \quad (3)$$

where B is the parameter that depends on the transition probability and $E_g^{opt.}$ is the optical energy gap. Finally, the electrical measurements were carried out by evaporating two gold planer electrodes ($14\times1\,mm^2$), using a conventional circuit involving a digital Keithley 617C electrometer.

3. Results and discussion

3.1. XRD and DSC analysis

Table 1 shows the calculated and measured chemical compositions of Ge_{15} Sb_{10} Se_{75} and $Ge_{25}Sb_{10}Se_{65}$ thin films. The estimated average precision was approximately 3% in the atomic fraction of each element.

Table 1
Spectral distribution for the constituent elements for $Ge_{15}Sb_{10}Se_{75}$ and $Ge_{25}Sb_{10}Se_{65}$ thin films

Specimen	Nominal composition at%			EDS results at%		
	Ge	Sb	Se	Ge	Sb	Se
$Ge_{15}Sb_{10}Se_{75}$	15	10	75	15.02	9.95	75.03
$Ge_{25}Sb_{10}Se_{65}$	25	10	65	25.03	9.93	65.04

XRD patterns have been investigated to obtain more information about structural changes, which are produced as a result of the annealing process of $Ge_xSb_{10}Se_{90-x}$ ($x = 15$ and 25 at%) thin films at different temperatures in the range 348–670 K (see Figs. 1 and 2). It is clear from these two figures that the as-deposited films are amorphous (Figs. 1a and 2a). Annealing of the as-deposited films for 2 h at a temperature 500 K for $Ge_{15}Sb_{10}Se_{75}$ and 630 K for $Ge_{25}Sb_{10}Se_{65}$ films shows few crystalline peaks of relatively low intensity, as shown in Figs. 1b and 2b. Further increase of annealing temperature to 550 and 680 K for both the films increases the peaks' intensity of crystalline phases (GeSe, $GeSe_2$ and Sb_2Se_3) as shown in Figs. 1c and 2c. Fig. 3 shows the DSC thermograms for $Ge_{15}Sb_{10}Se_{75}$ and $Ge_{25}Sb_{10}Se_{65}$ chalcogenide glasses recorded at a uniform heating rate 10 K/min. As shown in this figure, there is a very small single endothermic peak. This peak is attributed to the glass transition temperature (T_g), which represents the strength or rigidity of the glass structure. Also, there is an exothermic peak originating from the amorphous–crystalline transformation. The exothermic peak has two characteristic points: the first is the onset temperature of

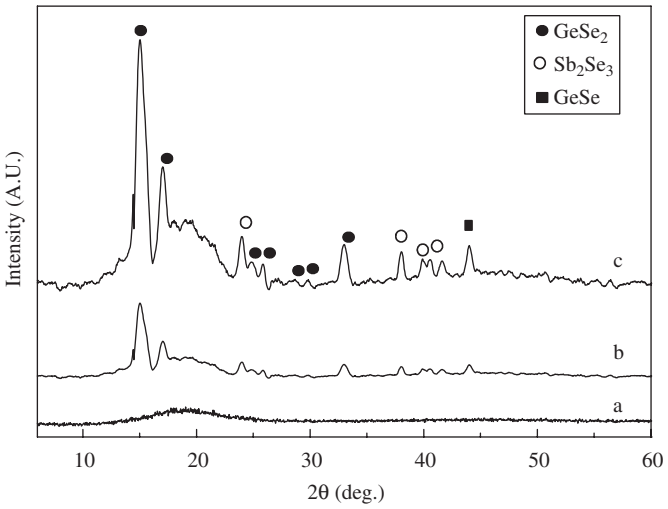

Fig. 1. X-ray diffraction patterns for (a) as-prepared, (b) annealed at 500 K and (c) annealed at 550 K for $Ge_{15}Sb_{10}Se_{75}$ thin films.

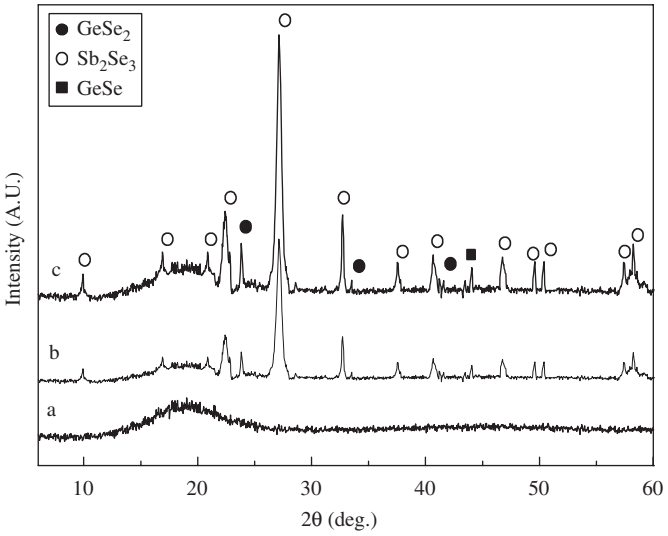

Fig. 2. X-ray diffraction patterns for (a) as-prepared, (b) annealed at 630 K and (c) annealed at 680 K for $Ge_{25}Sb_{10}Se_{65}$ thin films.

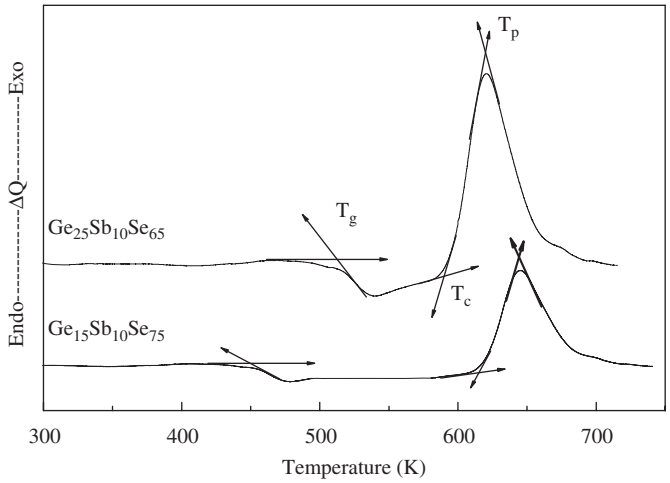

Fig. 3. DSC thermograms for the as-prepared $Ge_{15}Sb_{10}Se_{75}$ and $Ge_{25}Sb_{10}Se_{65}$ chalcogenide glasses recorded at 10 K/min.

crystallization (T_c) and the second is the temperature corresponding to the maximum crystallization rate (T_p). The glass transition temperature (T_g) is 445 and 503 K for the two compositions, respectively. It is clear from Fig. 3 that the increase of Ge content results in an increase of the value of T_g due to the increase of orderness and the lowering entropy of these glasses, while the crystallization peak temperature decreases with increasing Ge content.

3.2. Optical and electrical properties

The measured transmission (T) and reflection (R) spectra for $Ge_xSb_{10}Se_{90-x}$ ($x = 15$ and 25 at%) thin films are shown in Fig. 4a and b for the as-deposited and annealed films in the temperature range 348–568 and 373–668 K for $Ge_{15}Sb_{10}Se_{75}$ and $Ge_{25}Sb_{10}Se_{65}$ films, respectively. It can be seen from these two figures that for both the transmission and the reflection process, there is an opposite behavior with the variation of wavelength (or incident photon energy). Also, the optical transmission for $Ge_xSb_{10}Se_{90-x}$ ($x = 15$ and 25 at%) thin films increases (i.e., blue shift of the optical absorption edge) with increasing annealing temperature up to the glass transition temperature ($T_a \leqslant T_g$) followed by a remarkable decrease (i.e., red shift of the absorption edge) due to further increase of annealing temperature (i.e. $T_a > T_g$).

3.2.1. Effect of annealing on the optical band gap ($E_g^{opt.}$) and activation energy for electrical conduction (ΔE)

Fig. 5a and b represents the plots of $(\alpha h\nu)^{1/2}$ versus $(h\nu)$ for the as-deposited and annealed films. It is observed that Tauc's relation [26,27] for the allowed non-direct transition successfully describes the optical absorption process in these films. The extrapolation of the linear portion of Tauc's plots to $(\alpha h\nu)^{1/2} = 0$ yields the values of the non-direct optical band gap ($E_g^{opt.}$). Fig. 5c shows the dependence of $E_g^{opt.}$ on the annealing temperatures for $Ge_xSb_{10}Se_{90-x}$ ($x = 15$ and 25 at%) thin films. From this figure, one can observe that the optical band gap shows a slight increase with an increase in annealing temperature (T_a) if $T_a \leqslant T_g$, then $E_g^{opt.}$ starts to decrease remarkably, where $T_a > T_g$.

It is well known that the optical and electrical properties of amorphous materials strongly depend on the short-range order in the amorphous state and the defects associated with it. According to the Davis and Mott model [28] for amorphous materials, the width of the localized tail states near the mobility edges of the band gap depends on the degree of disorder and the density of

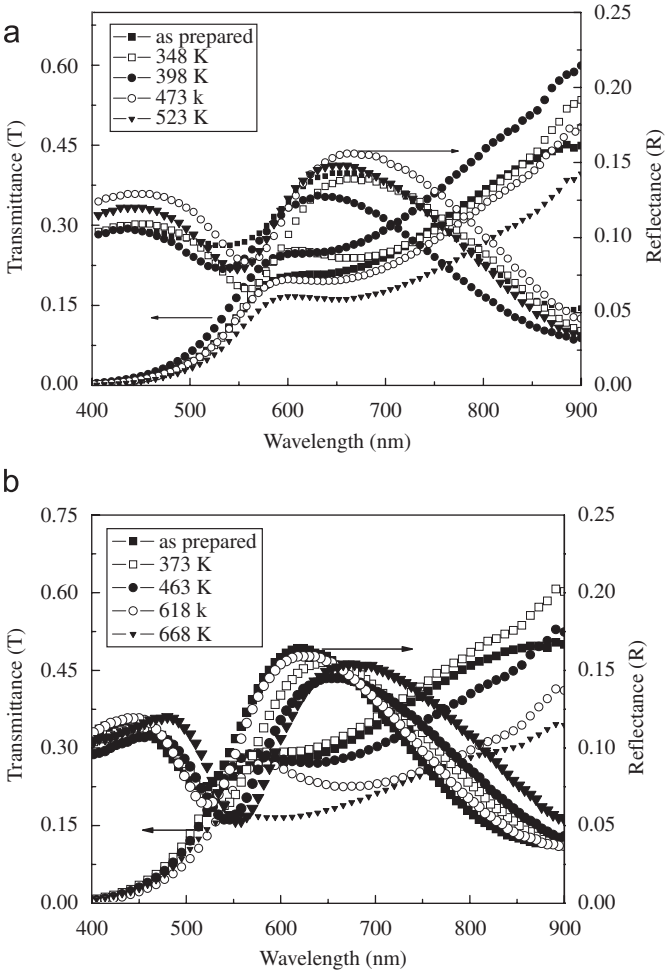

Fig. 4. (a) Transmittance and reflectance spectra for the as-prepared and annealed $Ge_{15}Sb_{10}Se_{75}$ thin films. (b) Transmittance and reflectance spectra for the as-prepared and annealed $Ge_{25}Sb_{10}Se_{65}$ thin films.

defects present in the amorphous state. In particular, it is known that unsaturated bonds together with some saturated bonds, such as like dative bonds [29], are produced as a result of an insufficient number of atoms deposited in the amorphous films [30]. Street et al. [31] proposed that thermally evaporated films are partially chemically disordered due to the presence of a large number of homo-polar bonds, whereas bulk glassy samples are chemically ordered. Furthermore, Hesegawa et al. [32] showed that the unsaturated bonds are responsible for the formation of localized tail states in the band gap. The presence of a high concentration of these states is responsible for the decrease of $E_g^{opt.}$ in the as-deposited films. This transformation is accompanied by an increase in grain size; therefore, the drastic effect of crystalline phases on optical gap can by explained as a result of the production of surface dangling bonds around the crystallites [33] during the crystallization process. Further increase of annealing temperature results in the breaking up of the formed crystallites into smaller crystallites, thereby increasing the number of surface dangling bonds responsible for the formation of some types of defects. These defects lead to the decrease of both the $E_g^{opt.}$ and ΔE values. The initial increase in the band gap due to the annealing of as-deposited films of $Ge_xSb_{10}Se_{90-x}$ glass at temperatures $T_a \leqslant T_g$ can be explained in terms of the density of the states model proposed by Mott and Davis [23] for amorphous materials. During thermal annealing, the unsaturated defects are gradually annealed out, producing a large number of saturated bonds [32]. These, in turn, reduce the density of localized states in

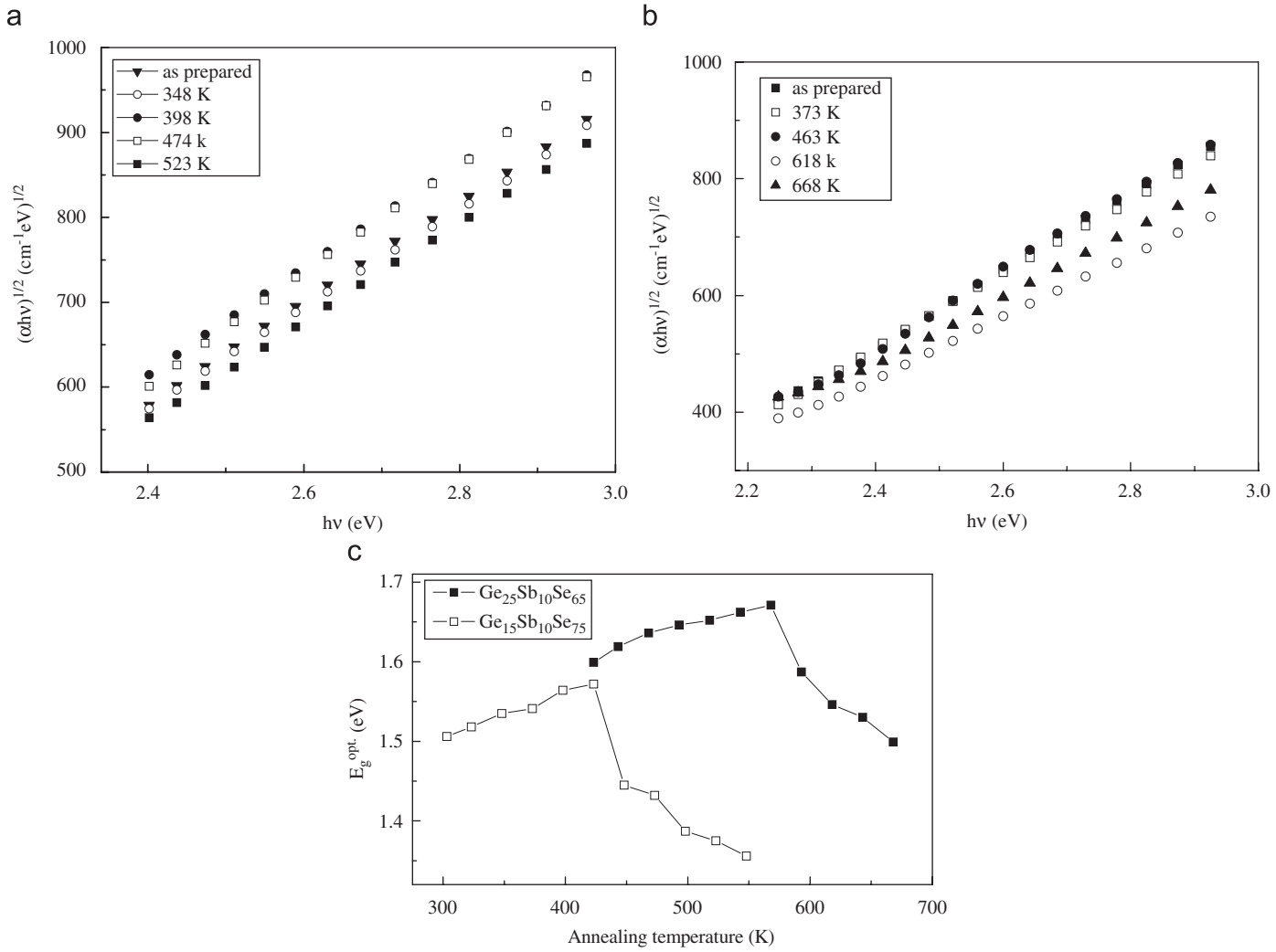

Fig. 5. (a) The plots of $(\alpha h\nu)^{1/2}$ vs. $h\nu$ for the as-prepared and annealed $Ge_{15}Sb_{10}Se_{75}$ thin films. (b) The plots of $(\alpha h\nu)^{1/2}$ vs. $h\nu$ for the as-prepared and annealed $Ge_{25}Sb_{10}Se_{65}$ thin films. (c) The effect of the annealing temperature on the optical band gap for $Ge_{15}Sb_{10}Se_{75}$ and $Ge_{25}Sb_{10}Se_{65}$ thin films.

the band structure and consequently increase in the values of both $E_g^{opt.}$ and ΔE. The observed decrease of both $E_g^{opt.}$ and ΔE for $Ge_xSb_{10}Se_{90-x}$ films where the annealing temperatures were higher than the glass transition temperature ($T_a > T_g$) can be explained as a result of amorphous to crystalline transformation. The three crystalline phases GeSe, $GeSe_2$ and Sb_2Se_3 were revealed due to the annealing process as shown in Figs. 1c and 2c. These figures show that the amount of crystalline phases in $Ge_xSb_{10}Se_{90-x}$ films increases with increase in the annealing temperature. These results are in a good agreement with many authors [15,16,34–36] and XRD patterns confirm our point of view concerning the annealing effects on the values of both the $E_g^{opt.}$ and ΔE for these films.

Furthermore, it was found that, $E_g^{opt.}$ for $Ge_{25}Sb_{10}Se_{65}$ is larger than $E_g^{opt.}$ for $Ge_{15}Sb_{10}Se_{75}$ films. This behavior can be explained in terms of the chemical ordered network model and (CONM) or the overall mean bond energy $\langle E \rangle$ of the $Ge_xSb_{10}Se_{90-x}$ system. (i) The shift of the average coordination number $z = 2.4$ for $Ge_{15}Sb_{10}Se_{75}$ glass to $z = 2.6$ for stoichiometric composition $Ge_{25}Sb_{10}Se_{65}$ of the $Ge_xSb_{10}Se_{90-x}$ system (where the deviation parameter (r) of stoichiometry equals 1 [37]) results in the increase of heteropolar Ge–Se bonds (long chains) at the expense of homopolar bonds (short chains); consequently, the value of the overall mean bond energy $\langle E \rangle$ of the system increases, since the energy of the Ge–Se single bond (55.2 kcal/mol) is greater than its value for the Se–Se single bond (44.04 kcal/mol); thereby $E_g^{opt.}$ increases. (ii) It is found that the increase of Ge content leads to an increase in the average coordination number (z) and glass transition temperature T_g as shown in Fig. 3. This increase of T_g results in lowering the entropy, i.e. decreasing the degree of randomness accompanied by the increase of $E_g^{opt.}$; (iii) According to the topological model [38], transition of an elastical (polymeric glass) 2D structure at $z = 2.4$ for $Ge_{15}Sb_{10}Se_{75}$ to a more rigid 3D order network structure (amorphous solid) may be one of the reasons affecting the value of $E_g^{opt.}$.

Fig. 6a and b represents the experimental dc conductivity $\ln(\sigma(T))$ versus T^{-1} for amorphous $Ge_{15}Sb_{10}Se_{75}$ and $Ge_{25}Sb_{10}Se_{65}$ films of thickness 200 nm at the temperature range 300–723 K. From these figures it is observed that the behavior exhibits one type of thermally activated conduction in this temperature range according to the well-known equation:

$$\sigma(T) = \sigma_o \exp^{-}\left(\frac{\Delta E}{K_B T}\right) \quad (4)$$

where σ_o is the pre-exponential factors including the charge carriers mobility and density of localized states, K_B is the Boltzmann's constant, T is the absolute temperature and ΔE is the corresponding activation energy, which is a function of

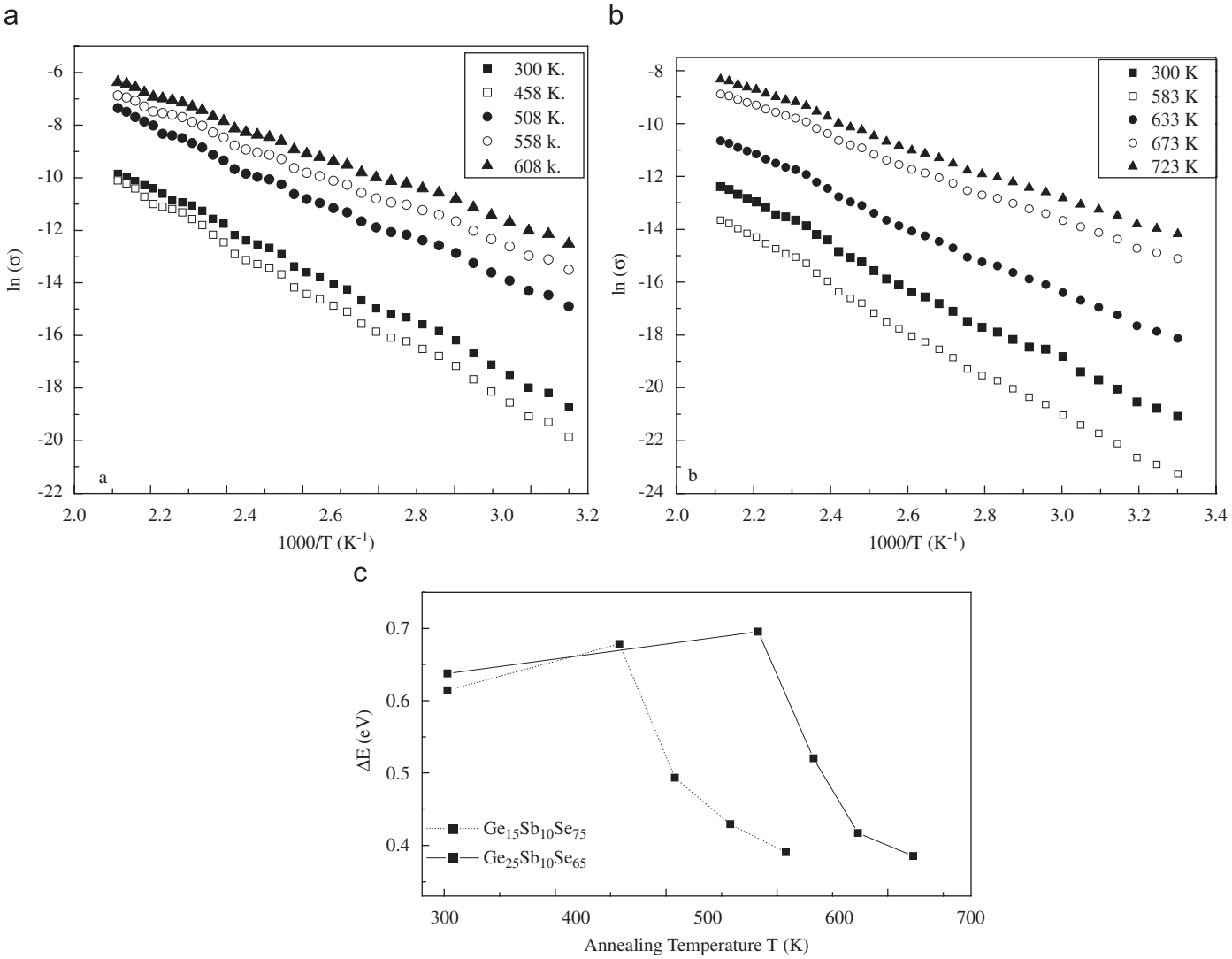

Fig. 6. (a, b). The plots of ln(σ) versus 1000/T for the as-prepared and annealed $Ge_{15}Sb_{10}Se_{75}$ and $Ge_{25}Sb_{10}Se_{75}$ thin films respectively and (c) the activation energy for electrical conduction (ΔE) as a function of the annealing temperature (T_a) for $Ge_{15}Sb_{10}Se_{75}$ and $Ge_{25}Sb_{10}Se_{65}$ thin films.

electronic energy levels of the chemically interacting atoms in the glass and hence the energy gap. Fig. 6a and b shows that the dark conductivity $\sigma(T)$ decreases with the increase of the annealing temperature up to T_g. This decrease in $\sigma(T)$ is accompanied by a slight increase in ΔE (Fig. 6c). At $T_a > T_g$, the conductivity increases, accompanied by a remarkable decrease in ΔE values with the increase of the annealing temperature. This effect of the annealing process on the values of ΔE is similar to that observed for $E_g^{opt.}$; (explained above), since ΔE is dependent on the $E_g^{opt.}$. The mechanism suggested to explain the conductivity in the range of temperature 300–723 K is based on the thermally dependent model of Mott and Davis [23], involving the presence of localized states originating from lack of long-range order and extending into the mobility gap, such that each of them activates the motion of carriers with a given range of temperature. The observed behavior of dc conductivity can be explained in terms of one of the two mechanisms: (i) the excitation of charge carriers into the extended states and (ii) the excitation of carriers into localized states near the band edges. The calculated values of $E_g^{opt.}$, ΔE and σ_o for the as-deposited and annealed films indicate that the first mechanism is most likely to explain the conduction process in $Ge_{25}Sb_{10}Se_{65}$ and $Ge_{15}Sb_{10}Se_{75}$ films [22,23].

4. Conclusions

The effect of heat treatment on optical and electrical properties of $Ge_{15}Sb_{10}Se_{75}$ and $Ge_{25}Sb_{10}Se_{65}$ thin films has been investigated in the range of annealing temperature 373–723 K. It was found that the allowed non-direct transition successfully describe the optical processes in these films. Both the optical band gap ($E_g^{opt.}$) and activation energy (ΔE) were increased with increasing annealing temperature (T_a) up to the glass transition temperature (T_g) and hence remarkable decrease in the values of ($E_g^{opt.}$) and (ΔE) occurred with further increasing of annealing temperature ($T_a > T_g$). This behavior was explained in terms of the Mott and Davis model for amorphous materials and amorphous to crystalline structure transformations. The annealing process at $T_a > T_g$ results in the formation of some crystalline phases GeSe, $GeSe_2$ and Sb_2Se_3 revealed in the XRD patterns, which confirms our discussion of the obtained results for the effect of heat treatment on optical band gap ($E_g^{opt.}$) and (ΔE).

References

[1] J.A. Savage, Infrared Optical Materials and their Antireflection Coating, A. Hilger, London 1985.

[2] A.E. Owen, A.P. Firth, P.I.S. Ewen, Pill. Mag. B 52 (1985) 347.
[3] S.R. Elliott, Physics of Amorphous Materials, Longman, New York, 1990.
[4] L. Tichy, H. Ticha, M. Frumar, J. Klikorka, A. Triska, C. Barta, A. Nemeckova, Czeeh, J. Phys. B 32 (1982) 1363.
[5] M.M. El-Sammanoudy, M. Fadel, J. Mater. Sci. 27 (1992) 646.
[6] H.W. Pinsler, W.E. Brower, J. Phys. Chem. Solids 38 (1977) 393.
[7] S.A. Fayek, S.M. El-Sayed, NDT&E Int. 39 (2006) 39.
[8] R. Vahalova, L. Tichy, M. Vleck, H. Ticha, Phys. Stat. Sol. A 181 (2000) 199.
[9] M. Vlcek, C. Raptis, T. Wagner, A. Vidourek, M. Frumar, I.P. Kotsals, D. Papadimitriou, J. Non-Cryst. Solids 192/193 (1995) 699.
[10] H.S. Metwally, Vacuum 62 (2001) 13.
[11] S. Mahadevan, A. Giridhar, A.K. Singh, J. Non-Cryst. Solids 57 (1983) 432.
[12] J. Vázquez, D. García-G. Barreda, P.L. López-Alemany, P. Villares, R. Jiménez-Garay, J. Alloys Compounds 421 (1–2) (2006) 109.
[13] A. Srinivasan, K.N. Madhusoodanan, E.S.R. Gopal, J. Philip, Phys. Pev. B 45 (1992) 8112.
[14] H.H. Moharam, Appl. Phys. A 66 (1998) 515.
[15] A.A. Abu-Sehly, J. Mater. Sci. 35 (2000) 2009.
[16] M.A. Abdel-Rahim, A.H. Moharam, M. Dongel, M.M. Hafiz, J. Phys. Chem. Solids 51 (1990) 355.
[17] M. Digiulis, D. Manno, R. Rella, P. Siciliano, A. Tepore, Sol. Energy Mater. 15 (1987) 209.
[18] M.M. Hafiz, A.H. Moharram, M.A. Abdel. Rahim, A.A. Abu-sehly, Thin Solid Film 292 (1997) 7.
[19] M.A. Abdel-Rahim, J. Phys. Chem. Solids 60 (1999) 29.
[20] J. Shiraguji, G.I. Kim, Y. Inuishi, J. Appl. Phys. 16 (1977) 67.
[21] A.S. Maan, D.R. Gopal, S.K. Sharma, T.P. Sharam, J. Non-Cryst. Solids 183 (1995) 186.
[22] N.F. Mott, Philos. Mag. 19 (1969) 835.
[23] N.F. Mott, E.A. Davis, Electronic Process in Non-Crystalline Materials, Clarendon, Oxford, 1979.
[24] E.A. Davis, N.F. Mott, Philos. Mag. 22 (1970) 903.
[25] H. Fritzsche, Philos. Mag. B 68 (1993) 561.
[26] O.S. Heavens, M.H. Liddell, Appl. Opt. 4 (1965) 629.
[27] M.H. Liddell, Computer-Aided Techniques for the Design of Multiayer Filters, Adam Hilger Ltd., Bristal, 1981.
[28] M. Vlect, C. Raptis, T. Wagner, A. Vidourck, M. Framar, I.P. Kotsalas, D. Papa dimitriou, J. Non-Cryst. Solids 192/193 (1995) 699.
[29] S.R. Ovshinsky, D. Adler, Contemp. Phys. 19 (1978) 109.
[30] M.L. Theye, in: Proceeding of the Fifth International Conference on Amorphous and Liquid semiconductors, Vol. I Garmisch–Partenkirchen, 1973, Taylor and Francis, London, 1973, p. 479.
[31] R.A. Street, R.J. Nemanich, G.A.N. Connel, Phys. Rev. B 18 (12) (1978) 6915.
[32] S. Hasegawa, S. Yazaia, T. Shimizu, Solid State Commun 26 (1978) 407.
[33] S. Choudhari, S.K. Biswas, J. Non-Cryst. Solids 54 (1983) 179.
[34] S. Hasegawa, S. Yasaki, Solid State Commun 23 (1977) 41.
[35] S. Hasegawa, M. Kitagawa, Solid State Commun 27 (1978) 855.
[36] S. Shegetomi, H. Ohkubo, Thin Solid Films 199 (1991) 215.
[37] L. Tichy, H. Ticha, J. Non-Cryst. Solids 189 (1995) 141.
[38] J.C. Phillips, J. Non-Cryst. Solids 34 (1979) 153.